

Global phosphoproteomic profiling reveals perturbed signaling in a mouse model of dilated cardiomyopathy

Uros Kuzmanov^{1,3,*}, Hongbo Guo^{1,*}, Diana Buchsbaum², Jake Cosme², Cynthia Abbasi², Ruth Isserlin¹, Parveen Sharma², Anthony Gramolini^{2,3,#}, and Andrew Emili¹

University of Toronto

Submitted to Proceedings of the National Academy of Sciences of the United States of America

Phospholamban (PLN) plays a central role in Ca²⁺ homeostasis in cardiac myocytes through regulation of the SERCA2A Ca²⁺ pump. An inherited mutation converting arginine residue 9 in PLN to cysteine (R9C) results in dilated cardiomyopathy (DCM) in humans and transgenic mice, but the downstream signaling defects leading to decompensation and heart failure are poorly understood. Here, we used precision mass spectrometry to study the global phosphorylation dynamics of 1887 cardiac phosphoproteins in early affected heart tissue in a transgenic R9C mouse model of DCM compared to wild-type littermates. Dysregulated phosphorylation sites were quantified after affinity capture and identification of 3908 phosphopeptides from fractionated whole heart homogenates. Global statistical enrichment analysis of the differential phosphoprotein patterns revealed selective perturbation of signaling pathways regulating cardiovascular activity in early stages of DCM. Strikingly, dysregulated signaling through the Notch-1 receptor, recently linked to cardiomyogenesis and embryonic cardiac stem cell development and differentiation but never directly implicated in DCM before, was a prominently perturbed pathway. We verified alterations in Notch-1 downstream components in early symptomatic R9C transgenic mouse cardiomyocytes compared to wild-type by immunoblot analysis and confocal immunofluorescence microscopy. These data reveal unexpected connections between stress-regulated cell signaling networks, specific protein kinases, and downstream effectors essential for proper cardiac function.

phospholamban | proteomic | bioinformatics | heart disease

INTRODUCTION

Cardiovascular diseases (CVDs) leading to systolic/diastolic heart failure (HF), such as hypertensive/diabetic heart disease, stroke and vascular atherosclerosis, are leading causes of death in the developed world (1). Many CVDs are associated with genetic predispositions. For example, in humans, the R9C substitution in phospholamban (PLN) has been shown to result in dilated cardiomyopathy (DCM) presenting in adolescence, leading to rapid deterioration of heart function and premature death (2). However, the etiology and molecular mechanisms of progression of DCM and other CVDs leading to HF are complex and still poorly understood, further complicating clinical assessment and management. From a biological and clinical perspective, the identification and characterization of clinically relevant, potentially druggable, pathways driving the maladaptive response in affected heart tissue is a key challenge to improved diagnostic and therapeutic tools for earlier detection and preventative treatment of both inherited and chronic CVDs.

Cardiac muscle contraction is controlled by Ca²⁺ flux and signaling relays, which are perturbed in HF. Internal stores of Ca²⁺ required for the proper functioning of cardiomyocytes (CMs) are normally maintained through the function of the sarco(endo)plasmic (SR) reticulum Ca²⁺-ATPase 2 (SERCA2) (3), which is responsible for the sequestration of Ca²⁺ resulting in muscle relaxation. SERCA2 activity is regulated through a reversible inhibitory interaction with PLN, which can be re-

lieved by phosphorylation of PLN by protein kinase A (PKA) or Ca²⁺/calmodulin-dependent protein kinase II (CaMKII) (3).

Proteomic analyses have revealed changes in the abundance of other effector proteins in diverse biochemical pathways in DCM. Notably, shotgun proteomic analysis of membrane protein expression dynamics in heart microsomes isolated from mice overexpressing a superinhibitory (I40A) mutant of PLN revealed changes in G-protein coupled receptor mediated pathways leading to activation of protein kinase C (PKC) (4). We previously reported quantitative changes in protein and cognate mRNA expression levels in cardiac ventricular tissue at different time points in the development of DCM in R9C-PLN mice representing clear clinical stages in the progression to HF (5). We showed that the latter maladaptive response was driven by elevated activity of MAPK signaling by the protein kinases p38 and JNK, in part through down-regulation of pro-survival microRNAs (6). However, the underlying upstream and downstream signaling events preceding HF were not fully explored.

In the present study, we report the first systematic, large-scale quantitative phosphoproteomic analysis of dysregulated protein phosphorylation-dependent signaling occurring at the early symptomatic stages of DCM progression in whole hearts from R9C mutant mice compared to wild-type littermates.

RESULTS

Comparative phosphoproteome analysis. To achieve a comprehensive survey of cardiac signaling cascades impacted by DCM, we performed global quantitative phosphopeptide profiling on

Significance

The present study demonstrates the utility of global phosphoproteomic profiling of diseased cardiac tissue to identify signaling pathways and other biological processes disrupted in cardiomyopathy. Perturbed Notch-1 signaling was identified by bioinformatics analyses of phosphoprotein patterns present in affected cardiac tissue in a transgenic mouse model system of dilated cardiomyopathy and by complementary molecular biology and microscopy techniques. In addition, dozens of other disturbed signaling pathways offer an opportunity for novel therapeutic and/or diagnostic clinically applicable targets. Although this study was performed in mice, only minor adjustments to the experimental approach would be required for comparative analysis of analogous samples from human cardiac patients, potentially leading to even more clinically relevant data.

Reserved for Publication Footnotes

137
138
139
140
141
142
143
144
145
146
147
148
149
150
151
152
153
154
155
156
157
158
159
160
161
162
163
164
165
166
167
168
169
170
171
172
173
174
175
176
177
178
179
180
181
182
183
184
185
186
187
188
189
190
191
192
193
194
195
196
197
198
199
200
201
202
203
204

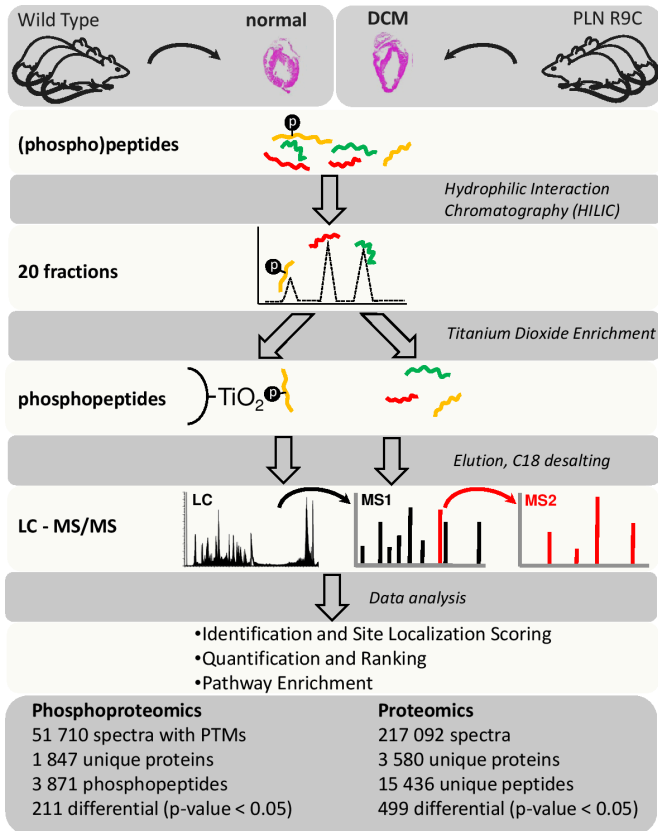


Fig. 1. General phosphoproteomics workflow. Three pooled hearts from R9C PLN transgenic and wild type littermates were analyzed by quantitative precision LC-MS/MS.

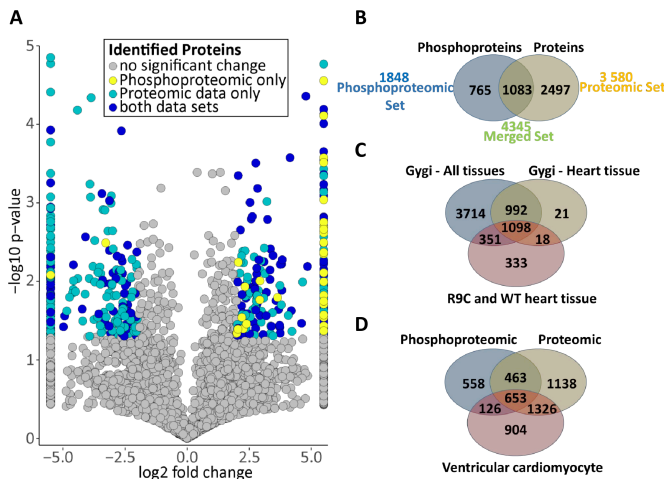


Fig. 2. (A) Volcano plot indicating significantly altered proteins and phosphoproteins identified in the combined data sets. Log-transformed p-values (t-test) associated with individual peptides and phosphopeptides plotted against log-transformed fold change in abundance between the PLN R9C and wild type hearts. (B) Venn diagram depicting the total number of proteins identified in the corresponding proteomic and phosphoproteomic datasets. (C) Venn diagram depicting phosphoprotein overlap with mouse tissue phosphoproteomes from Huttlin et al. (63). (D) Venn diagram depicting overlap of R9C and WT combined phosphoproteome and proteome with ventricular cardiomyocyte proteome from Sharma et al. (12).

three independent biological replicates of whole heart tissue isolated from 8-week old (early symptomatic) R9C mice and wild-

type littermates. A major experimental consideration was preservation of phosphorylation site integrity, through use of phosphatase inhibitors, low temperature, and harsh denaturing sample processing conditions. To achieve the deepest possible coverage, we performed chromatographic sample pre-fractionation steps, using hydrophilic interaction liquid chromatography (HILIC) to separate peptides bearing negatively charged phosphate moieties (7). Given the low relative abundance of phosphopeptides and their tendency to be undetectable due to ion competition/suppression during MS analysis, we performed differential affinity capture with immobilized metal oxide affinity chromatography (TiO₂) to enrich for phosphopeptides. To measure differences in relative abundance, we applied label-free quantification, comparing the extracted parent ion current intensities recorded in high-energy collision dissociation (HCD) spectra using a high precision Orbitrap instrument. In parallel, we measured total protein levels by shotgun sequencing.

In total, our stringent data analysis workflow (Fig S1) mapped 94,956 and 217,092 spectra to mouse reference protein sequences for the phosphoproteomic and background proteomic data sets, respectively. From this, we derived a set of high-confidence sequence matches (FDR ~1% at both protein and peptide levels) corresponding to over 1,800 cardiac phosphoproteins and 3,900 phosphopeptides in normal and DCM hearts, and 15,436 unique peptides mapping to 3,580 unique proteins in the background proteomic data set (Fig S1, Fig 2A/B). For the former, we confidently (site localization probability >0.7 as described in Supp. Methods) identified 7,589 unique putative phosphorylation sites (i.e. sites on identified phosphopeptides with supporting MS/MS data and localization probability greater than 0.7) of which 6,855 mapped to serine, 674 to threonine, and 60 to tyrosine residues (consistent with the expected 90:9:1% cellular distribution ratios) on 1,848 distinct cardiac proteins (Fig 2A/B; see Supp. Datasets S1 and S2). Our coverage is comparable to a pioneering study of the mouse cardiac phosphoproteome by Lundby et al. (8) and a recent phosphoproteomic analysis of *in vivo* effects of CaMKII inhibition in mouse hearts (9). Phosphoproteins identified in our study also showed considerable overlap with heart and other tissue profiles in the mouse phosphoproteomic atlas reported by the Gygi group (10), but 333 were uniquely identified in our study; 96 of which contained phosphopeptides significantly altered and/or solely identified in R9C hearts (Fig 2C). A high degree of overlap with the mouse ventricular myocyte proteome by Sharma et al. (11) was also observed (Fig 2D).

Quantification and Ranking. Based on reproducible measurements of precursor ion intensity, we scored both the individual phosphopeptides and their consolidated cognate phosphorylation sites for differential relative abundance between the healthy and diseased samples. Based on a two-tailed student's t-test ($p < 0.05$), the abundance of 211 phosphopeptides was differentially altered (elevated or reduced) between the R9C and WT hearts (Fig 2A; see Supp. Dataset S1), with 86% of these predominantly higher in the disease state. In comparison, 499 proteins showed differential expression, consistent with our previous report (5).

Systematic evaluation of the corresponding biological annotations revealed the aberrant phosphorylation patterns occurred on proteins linked to disparate subcellular compartments, ranging from membrane-associated receptors to nuclear-localized proteins with established links to heart development, contractile function and/or cardiomyopathy (Supp. Data 1). Consistent with expectation, the predominant phosphoform of PLN detected preferentially in R9C hearts was phosphorylated on serine 16, a site critical for inhibition of SERCA2 activity (3). We also detected alterations in the phosphorylation pattern of central kinases involved in cardiac signaling like protein kinase A (PKA). Additionally, the S112 site on the PKA Type II regulatory beta

205
206
207
208
209
210
211
212
213
214
215
216
217
218
219
220
221
222
223
224
225
226
227
228
229
230
231
232
233
234
235
236
237
238
239
240
241
242
243
244
245
246
247
248
249
250
251
252
253
254
255
256
257
258
259
260
261
262
263
264
265
266
267
268
269
270
271
272

273
274
275
276
277
278
279
280
281
282
283
284
285
286
287
288
289
290
291
292
293
294
295
296
297
298
299
300
301
302
303
304
305
306
307
308
309
310
311
312
313
314
315
316
317
318
319
320
321
322
323
324
325
326
327
328
329
330
331
332
333
334
335
336
337
338
339
340

341
342
343
344
345
346
347
348
349
350
351
352
353
354
355
356
357
358
359
360
361
362
363
364
365
366
367
368
369
370
371
372
373
374
375
376
377
378
379
380
381
382
383
384
385
386
387
388
389
390
391
392
393
394
395
396
397
398
399
400
401
402
403
404
405
406
407
408

Table 1.

motifs	Kinase	MOTIF SCORE	matches	fold increase
...RS.S.....	CamKII, PKA, PKC, CK2	27.34	59	4.76
.....SD.E...	CK2	24.66	34	6.77
....SPT.....	GSK3, ERK1/2, CDK5, CK2, DNA-PKcs	23.7	27	7.75
.R..S.S.....	CamK2, PKA, PKC, CK2	23.62	34	5.64
....SDS.....	CK2, BARK	17.65	21	6.41
.....SP...	GSK3, ERK1/2, CDK5	16	275	2.34
...S..S.....	CK1, CK2	16	258	1.74
...R..S.....	CamK2, PKA, PKC	12.45	123	2.01
.....TP.....	GSK3, ERK1/2, CDK5	9.46	63	2.35
..S...S.....	GPCRK1, MAPKAPK2K, GSK3	8.1	120	1.7

Top 10 ranked identified consensus motifs on phosphopeptides significantly altered and/or exclusively detected in R9C heart tissue with kinases predicted to target these sequences. Number of matches in the query set and fold increase over the normal occurrence of consensus sequence is also provided.

Submission PDF

Table 2.

Pathway	Identified components	Cardiac Context
Notch-1 signaling	hdac7(s178), tle3(s216), snw1(s224,s232), tmed2, ncor2*, tbl1xr1, tbl1x, ncor1(s2351), ep300, adam10, crebbp, rbx1, numb, hdac5(s652), arrb1, rps27a, mib1	dilated cardiomyopathy, left ventricular non-compaction, cardiac development (36, 40)
VIP signaling	map3k1(s915), ppp3cb(s469), plcg1(s1263), nfatc2(s136), prkar2b(s112), prkachb, prkar2a, prkar1a, nfkb1, ppp3ca	myocardial fibrosis, diabetic cardiomyopathy, ischemia-reperfusion (41)
H3-K4 Histone methylation	ogt, kmt2a, snw1(s224,s232), nipbl(s2652), bcor(s423), men1, kdm1a, mt2b, dnmt1*, pml(s449), pygo2(t264), ctbp1, arrb1, ube2n, wbp2, lpin1	hypertrophic cardiomyopathy, fetal gene program (42)
BCR signaling, beta cell activation and regulation	mif, irs2(s1165), thoc1(s560), sos1*, orai1, fas*, sash3*, ptpnc3(s801), lyn(s19), syk, itpr1(s1573), cd81, stim1*, ptpn6, nfatc2(s136), inpp5d(t701,s709), sh3kbp1(s193), aplf(s41), cbl, plcg1(s1263), tcf3(s517), bad(s112), itpr2, calm1, pawr, itpr3, bmi1, nck1	heart failure, hypertrophy, myocardial fibrosis, myocardial infraction, ischemia-reperfusion (43, 44)
TGFb/smad signaling	glg1, pdpk1(s117), jun(s63), lemd3, fbn2, men1, zeb1, aspn, eng, snx6, zfyve9, cav3, sptbn1, bcl9l, strap, cav2*, ppm1a, htra1	dilated cardiomyopathy, heart failure, fibrosis, myocardial infraction, cardiac remodeling (24, 45)
PPARa signaling	med19(s226), txnrd1, ankrd1, wwtr1*, abca1(s2234), yap1, med24*, tbl1xr1, alas1, cdk19, tbl1x, apoa1, acox1, apoa2, smarcd3, agt, ncoa3*, ncoa2, nfya(s187), fh12, sp1, ncoa6, acadm, acsl1, cd36, crebbp, slc27a1, cpt2, ncor1(s2351), plin2, me1, ep300	dilated cardiomyopathy, heart failure, diabetic cardiomyopathy (24, 46)
TLR signaling	hsp90b1(s306), lgmn, ikkbb, map2k1, app, nfkb2(t425), dhx9(s137), dnm2, ppp2r5d*, unc93b1, dnm1(s774), itgb2, rps6ka3, eea1, dusp3, tlr3, ctsb, nfkb1, ube2n, ppp2ca, cd36, mef2a, ppp2r1a	dilated cardiomyopathy, heart failure, ischemia-reperfusion, hypertrophy, viral myocarditis (24, 47)
Wnt signaling	scyl2(s253), dab2ip(s854), ranbp3, cdh2, wwtr1*, rapgef1*, gsk3a, ppp2r3a, mcc*, dab2, limd1, cttnb1, dact3(s165), bicc1, gsk3b, stk3(s246), ctndd1(s813), g3bp1, cav1, ppp2r5a, pi4k2a(s462), cul3, mapk14*, dvl3*, hdac2(s394)	dilated cardiomyopathy, fibrosis, heart failure, myocardia infraction, arrhythmia (24, 48)

List of select cardiac-relevant signaling pathways (from the Cytoscape analysis), along with their relevant protein components, altered in R9C PLN hearts. Phosphopeptides/proteins increased in R9C hearts are shown in bold, while components identified but showed a decrease in R9C are not bolded. The identified phosphorylation site of a particular protein is indicated in brackets. Proteins annotated with * are 'ambiguous' as described in methods. For a full list of protein/gene names associated with each pathway, refer to Supp. Data.

409
410
411
412
413
414
415
416
417
418
419
420
421
422
423
424
425
426
427
428
429
430
431
432
433
434
435
436
437
438
439
440
441
442
443
444
445
446
447
448
449
450
451
452
453
454
455
456
457
458
459
460
461
462
463
464
465
466
467
468
469
470
471
472
473
474
475
476

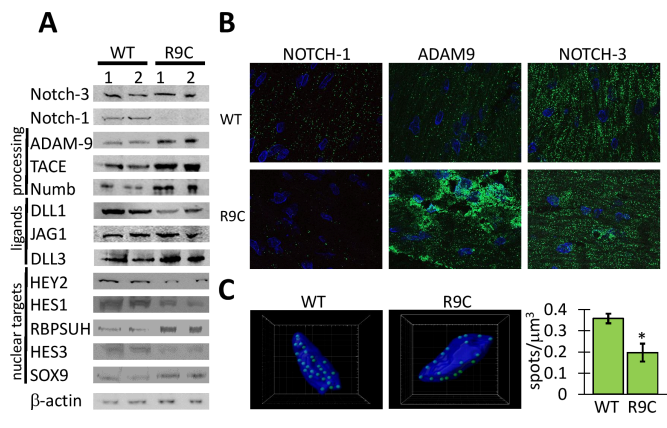


Fig. 3. (A) Immunoblots of components of the Notch-1 signaling pathway. **(B)** Immunofluorescence images of Notch-1, ADAM9, and Notch-3 in ventricular sections of WT and R9C PLN hearts. **(C)** Representative reconstructed images showing nuclear localization of the Notch-1 intracellular domain and bar graph showing quantification of relative distribution (spots identified/nuclear volume as determined by Hoechst staining) in WT and R9C PLN hearts (p -value = 0.00282).

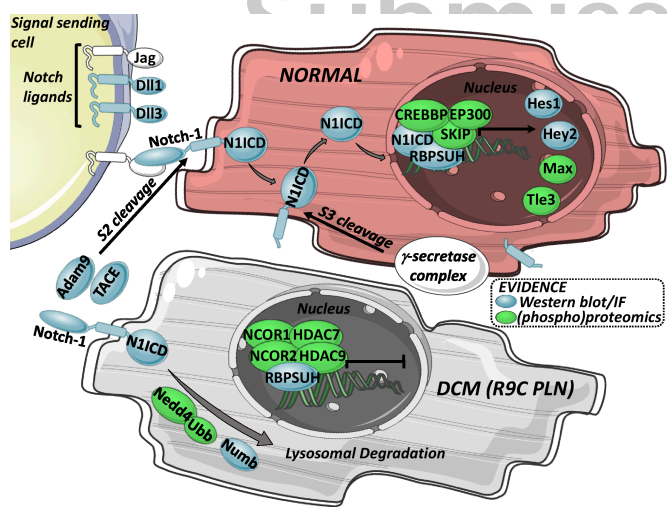


Fig. 4. Proposed schematic model of Notch-1 signaling in normal and DCM cardiomyocytes populated with differential proteins identified with different lines of evidence in whole heart lysates or ventricular sections, including: proteomic data, phosphoproteomic data, immunoblotting, and immunofluorescence.

subunit (PRKAR2B), which results in the lowering of the activation threshold of PKA (12), increased in R9C. Additionally, we detected abundance changes in cardiac stress markers (FHL1), indicators of the fetal gene program (MYH7), markers of ECM remodeling (POSTN, SPARC), and proteins involved in Ca^{2+} modulation (SLMAP, CASQ2) (Supp. Datasets S1 and S2).

Further examples of interest include the highest ranked phosphorylated peptide (S64 + T69) from eIF4E binding protein 1 (EIF4EBP), which negatively regulates translation initiation. Hypophosphorylated EIF4EBP acts as a repressor of eIF4E, whereas its phosphorylation releases eIF4E, thereby upregulating protein translation in response to signaling by diverse cell surface receptors, including insulin, EGF, PDGF and other ligands (13). In heart, EIF4EBP has been implicated in ischemia-reperfusion stress, cardiomyocyte survival, cardiac hypertrophy, and oxidative and nutritional stress responses (13).

Also significantly more highly phosphorylated in R9C hearts was a previously uncharacterized T187 site in EMMPRIN (BSG/CD147), an extracellular metalloprotease inducing mem-

ber of the immunoglobulin superfamily, consistent with its role in inflammatory processes in cardiac remodeling (14). In addition, the S2 phosphosite on transcription factor MAX (Myc associated factor X) (15), a positive regulator of cardiac alpha-myosin heavy-chain gene expression in cardiomyocytes, was significantly altered in R9C mice. Phosphorylation of S2 inhibits DNA binding by MAX homodimers and association with MYC, but is not known to affect its interaction with another cofactor, transcription enhancer factor 1 (TEF-1, TEAD1), or regulation of cardiac alpha-myosin heavy chain (16). In contrast, when phosphorylated, the S73 site of transcription factor JUN, likewise more highly phosphorylated in the R9C mutant mice, is linked to increased transcription of JUN target genes encoding components of a myriad of signaling pathways (17).

Phosphosites on two intercalated disc-associated Xin repeat proteins (XIRP1, XIRP2) with roles in cardiac development were also increased significantly in R9C hearts. XIRPs interact with catenins and ion channels in mature cardiac muscle and while the significance of phosphorylation is unclear, gene knock out mice display early onset cardiomyopathy (18).

Kinase Target Motif Analysis. We used the MotifX algorithm (19) to identify consensus motifs overrepresented in the set of phosphopeptides identified exclusively in R9C heart tissue and/or those showing significant ($p < 0.05$) differential expression between R9C and wild-type mice (Table 1 and Supp. Dataset S1). Candidate consensus sequences were processed using PhosphoMotif Finder (20) to identify cognate kinases known or predicted to phosphorylate these sequences.

We found central kinases involved in cardiac contractility through transient Ca^{2+} regulation among the most overrepresented compared to the whole mouse proteome. Two consensus motifs identified were targeted by PKA and CaMKII (Table 1), one enriched 4.76-fold (59 matches) over background and the other 5.64-fold (34 matches). Phosphorylation of PLN by PKA on S16, or by CaMKII on T17, reverses PLN-mediated inhibition of SERCA2a activity up to 3-fold during β -adrenergic stimulation (3). Upregulation of these kinases is expected as a compensatory mechanism considering that R9C-PLN mutant molecules effectively trap PKA, inhibiting phosphorylation of wild-type protein and relieving SERCA2a inhibition (2).

Two consensus sequences targeted by extracellular signal regulated kinases (ERK1/2) were identified on 275 significantly altered phosphopeptides (Table 1). ERK1/2 becomes activated in cardiac myocytes in response to a variety of stimuli, including progression of DCM (21). Likewise, we found consensus motifs associated with phosphorylation by casein kinases and GSK3 kinases, previously linked to cardiac pathology (22).

Pathway Network Enrichment Analysis. For each phosphoprotein (and corresponding gene), the most differential peptide or modification site was selected for a systematic pathway enrichment analysis (see Methods). Phosphopeptides were initially ranked based on the level of statistical significance (differential p -value) rather than direction (up/down) of observed fold change. The focus of this analysis was to identify pathway-level alterations present in R9C mice compared to controls.

Three sets of enrichment analyses were performed to gain the most complete coverage, based on: (i) ranking the phosphoproteomic data set alone, (ii) the background proteomic data set alone, and (iii) a merged combination of both (Fig 2A/B and Supp. Fig S1), which included the significant differentially abundant proteins derived from both the proteomic background and differential phosphorylation events. This merged set of 4,345 unique proteins/genes (Fig 2B) was included since signaling perturbations do not necessarily consist only of changes in phosphorylation state or protein expression alone, but often rather both in concert. The most differentially expressed peptides or phosphorylation events (based on p -value) from each protein

545 were used to represent individual protein/gene products. The
546 majority of enriched pathways found in the merged set (**Supp.**
547 **Dataset S3**) reflected the presence of many proteins exclusively
548 in the background proteome. Of the 2,039 gene sets enriched in
549 the merged set, many (1,427) were likewise enriched in the global
550 proteomic data alone (**Supp. Fig S1**).

551 We chose to focus on a subset of 612 pathways and processes
552 that reflected contributions from both datasets, rather
553 than merely differential protein levels. To simplify analysis by
554 minimizing redundancy in the annotation term labels (**Supp.**
555 **Data S1**), we combined the 182 enrichments from the phospho-
556 proteomic data set (not in the background proteome) with the
557 526 gene sets unique to the merged set (**Supp. Fig S1** and
558 **Dataset S3**). By visualizing the resulting 708 enriched gene sets
559 as a single graphical Enrichment Map (23), we identified several
560 dysregulated pathways of notable relevance to cardiac pathology
561 (**Table 2, Supp. Fig S2**). For instance, reflecting a central
562 role in cardiac physiology and pathology, dysregulated pathways
563 associated with activation PKA and cAMP-dependent kinases
564 were prominently overrepresented in all gene set enrichment
565 analyses (**Supp. Datasets S1 and S3**). Considering the ubiquity
566 of many signaling pathways across different tissues and cell types,
567 when examined as a whole (rather than individual components),
568 it is not surprising that most pathways have associations with
569 other disorders or processes. This is also partly a bias of existing
570 annotations in curation databases.

571 To identify disease signatures specifically relevant to DCM,
572 we integrated and compared these pathways against a recent in
573 depth RNAseq-based gene expression study of the R9C PLN
574 model (**Supp. Datasets S2 and S6**) (24). Specifically, differential
575 mRNA expression modules in the Seidman study corresponding
576 to cardiomyocyte and non-myocyte cardiac cell populations
577 at different stages of disease (represented by six individual
578 nodes) were tested for overlap with our enrichment map using
579 a stringent Mann-Whitney test cutoff ($p < 0.01$). Strikingly, we
580 observed highly significant overlap between most of the disrupted
581 biological processes and signaling pathways noted by the two
582 studies, including (but not limited to): innate immunity, glucose
583 metabolism, TGF beta signaling, PPAR signaling, Wnt/ β -catenin
584 signaling, and TLR signaling. Notably, the general pathways involved
585 in metabolic and pro-fibrotic processes determined by the
586 Seidman study to differentiate between DCM and hypertrophic
587 cardiomyopathy (HCM) were likewise detected as differentially
588 perturbed in R9C hearts in our merged data.

589 **Notch-1 Signaling.** Distinct from the Seidman study, however,
590 we identified evidence for significant disruption in homeostatic
591 Notch-1 signaling in R9C hearts, with most phosphosites
592 never reported before in the context of DCM. For instance,
593 uncharacterized sites on SNW1 and CREBBP, members of the
594 Notch-1 transcription co-activator complex (25), were hyperphosphorylated
595 in the R9C mice. Similarly, we detected previously unreported
596 phosphorylation sites on both MAX and NCOR1 and NCOR2,
597 components of a downstream transcriptional co-repressor complex
598 known to inhibit transcription of Notch target genes (26).

600 To directly determine the differential state of Notch receptor
601 signaling, we performed immunoblots (**Fig 3A**) using a panel
602 of antibodies targeting different Notch receptor isoforms
603 (Notch1/3), activating and inhibiting ligands (DLL1/4, JAGG1/2,
604 NUMB), processing enzymes (ADAM9/17), and key downstream
605 effector transcription factors (HEY2, HES3, SOX9). Strikingly, a
606 very substantive and specific decrease in total Notch-1 receptor
607 levels was seen in the R9C hearts, while levels of Notch-3 receptor
608 were unchanged (Notch-2 was undetectable, as was the cleaved
609 Notch-1 intracellular domain).

611 Of the activating Notch ligands, DLL1 was downregulated in
612 R9C, while JAGG1 showed no change (DLL4 and JAGG2 were

613 not detected). Conversely, DLL3 and NUMB, which can suppress
614 Notch signaling, were upregulated in R9C hearts. Two metallo-
615 proteinases (ADAM9 and TACE/ADAM17) required for extra-
616 cellular processing and/or degradation of the Notch-1 receptor
617 were similarly upregulated in R9C. Conversely, the downstream
618 Notch-1 regulated transcription factors HES1 and HEY2 were
619 downregulated in R9C.

620 Immunofluorescence visualization of components of the
621 Notch signaling pathway in ventricular wall of R9C and wild-type
622 hearts (**Fig 3B**) established downregulation of Notch-1 receptor
623 expression in R9C cardiomyocytes along with upregulation of the
624 ADAM9 metalloproteinase (Notch-3 was unchanged). Imaparis-
625 based quantification (**Fig 3C**) of signal intensity and localization
626 of the Notch-1 intracellular domain (NICID) in cardiomyocyte
627 nuclei, indicative of Notch-1 activation, revealed a significant decrease
628 ($p < 0.003$) in overall nuclear localization of NICID in cells
629 in the ventricular sections of R9C hearts compared to controls
630 (due to gross changes in tissue morphology in R9C hearts, a large
631 proportion of nuclei showed no NICID colocalization). These
632 results verify Notch-1 receptor signaling inhibition in affected
633 heart tissue during early-stage disease (**Fig 4**).

634 DISCUSSION

635 During pathological cardiac remodeling, including DCM, dis-
636 ruptions in various signaling cascades have been reported, in-
637 cluding AKT, ERKs, GSK-3, JAKs, MAPKs, PI3K, PKA, PKC,
638 and TGF β . Activation or inhibition of signaling pathways can
639 ultimately result in changes to cardiomyocyte cell growth, differ-
640 entiation, proliferation and/or survival (27). Yet despite advances
641 in understanding the molecular basis of cardiac disease, a clear
642 global picture of system wide signaling network perturbations
643 does not exist for most conditions, including DCM. To address
644 this gap, we applied quantitative precision mass spectrometry to
645 glean the complex interplay of signaling events associated early
646 during disease progression with a genetic cause of cardiac HF.

647 One third of all cardiac proteins are known or predicted to
648 be phosphorylated. Here, we mapped 7,589 phosphopeptides on
649 1,848 cardiac proteins, of which 211 were differentially abundant
650 in the R9C model, providing unprecedented insights into the
651 global dysregulation of signaling cascades in early-stage DCM.
652 Many sites we identified are novel and of unknown biological
653 significance. While annotated repositories of experimental
654 phosphoproteomic datasets have been established (e.g. Phospho-
655 SitePlus) (28), establishing relevance to heart biology and
656 CVD is not straight-forward. Our present study aimed to first
657 identify significantly altered individual phosphosites and then use
658 the corresponding associated protein/gene annotations in con-
659 junction with information gained from global proteomic analysis.
660 This design was motivated by computational tools for signaling
661 network analysis and visualization, which historically focused on
662 gene expression datasets rather than individual phosphosites.

663 One especially intriguing finding was identification of Notch-
664 1 signaling as prominently altered in DCM. The Notch pathway
665 is a widely studied system crucial to "cell fate" determination
666 (29). Mammals express four Notch receptors (Notch 1-4) and five
667 ligands (DLL-1, -3, -4, JAGG-1, -2) (30). Notch-1 is expressed
668 across a broad variety of cell types, including cardiomyocytes.
669 All members of the Notch family are translated as single chains,
670 but are subsequently processed in the Golgi system to produce
671 extracellular and transmembrane subunits that remain bound
672 together at the plasma membrane by non-covalent bonds. Gen-
673 erally, ligand binding triggers the selective cleavage and removal
674 of the extracellular subunit by members of the ADAM protease
675 family, followed by cleavage of the membrane-bound intracellular
676 subunit by γ -secretase to release NICD, which translocates to
677 the nucleus to modulate transcription (**Fig 4**). However, this
678 oversimplification does not reflect cell context as different ligands
679
680

681
682
683
684
685
686
687
688
689
690
691
692
693
694
695
696
697
698
699
700
701
702
703
704
705
706
707
708
709
710
711
712
713
714
715
716
717
718
719
720
721
722
723
724
725
726
727
728
729
730
731
732
733
734
735
736
737
738
739
740
741
742
743
744
745
746
747
748

can act as Notch inhibitors, while processing enzymes can oppose Notch activation (29).

Changes in phosphorylation of Notch signaling components included an uncharacterized phosphorylation site on the polyubiquitin protein UBB required for homeostatic recycling of Notch-1, which is upregulated in R9C mice (31), as well as members of the histone deacetylase family (HDAC-4, -7, -9) and others (32). However, due to incomplete functional annotation, our cautious conclusion was that Notch-1 pathway was disrupted but not the precise nature of the perturbation (i.e. activation/inhibition).

We verified changes in Notch-1 signaling by immunoblots and immunofluorescence. We demonstrated downregulation of Notch-1 and DLL1 in R9C. DLL3, a Notch-1 ligand previously shown as a cis-acting inhibitor (33), was upregulated along with NUMB, whose association with Notch-1 leads to proteasomal degradation (34). ADAM9 and TACE/ADAM17, normally necessary for activation of Notch-1, were also upregulated in R9C. However, excessive expression of these proteases has also been shown to inhibit Notch signaling, while deficiency of a major associated inhibitor, TIMP3, leads to dilated cardiomyopathy in mice (35). Furthermore, expression and nuclear localization of the NICD domain of Notch-1 were significantly greater in wild-type cardiomyocytes compared with R9C. Together, these results show that Notch-1 signaling is downregulated in myocardium in early-stage DCM.

Our findings are consistent with previous reports of development of DCM *in vitro* and in newborn mice treated with an inhibitor of Notch-1 dependent signaling (36), or more pronounced cardiac dysfunction, fibrosis and apoptosis in adult

hearts from an agonist-induced hypertrophy model or Notch-1 cardiac-specific null mice (37). Similarly, transgenic mice overexpressing Notch ligand, JAGGED1, were protected from pressure overload-induced cardiac hypertrophy (38).

Considering this unprecedented phosphoproteomics data, it is clear that a more complete understanding of Notch-1 signaling and other potentially relevant pathways in adult heart following injury, including human patients, is warranted (39). Indeed, uncoupling of Notch-1 signaling in R9C (Fig 4) suggests that Notch-1 activating compounds (i.e. activating antibodies, polypeptides, small molecules) may be clinically beneficial under DCM conditions, similar to that observed in hypertrophy (38) and potentially other pathological contexts.

MATERIALS AND METHODS

Transgenic mice carrying the R9C mutation in the PLN gene were previously described (2). Workflows for heart sample preparation, processing and (phospho)proteomic profiling, including chromatographic fractionation, MS data generation, phosphosite localization and scoring, statistical enrichment analyses, motif prediction, Western blotting, and immunofluorescence, are detailed in the **Supp. Methods** available online.

Acknowledgements

We thank Paul Taylor, Peter Backx, Gary Bader, Michael Moran and David H. MacLennan for valuable advice. This project was funded by the Heart and Stroke Foundation of Ontario (T-6281) to AOG; the Canadian Institutes of Health Research to AOG (MOP-106538); the Ontario Research Fund (Global Leadership in Genomics and Life Sciences grant GL2-01012) and Heart and Stroke Richard Lewar Centre to AOG and AE; AOG is a Canada Research Chair in Cardiovascular Proteomics and Molecular Therapeutic. AE is the Ontario Research Chair in Biomarkers Of Disease Management. UK received Postdoctoral Fellowship support from the Ted Rogers Centre for Heart Research.

1. Mozaffarian D, et al. (2015) Heart disease and stroke statistics--2015 update: a report from the American Heart Association. *Circulation* 131(4):e29-322.
2. Schmitt JP, et al. (2003) Dilated cardiomyopathy and heart failure caused by a mutation in phospholamban. *Science* 299(5611):1410-1413.
3. MacLennan DH & Kranias EG (2003) Phospholamban: a crucial regulator of cardiac contractility. *Nat Rev Mol Cell Biol* 4(7):566-577.
4. Pan Y, et al. (2004) Identification of biochemical adaptations in hyper- or hypocontractile hearts from phospholamban mutant mice by expression proteomics. *Proc Natl Acad Sci U S A* 101(8):2241-2246.
5. Gramolini AO, et al. (2008) Comparative proteomics profiling of a phospholamban mutant mouse model of dilated cardiomyopathy reveals progressive intracellular stress responses. *Mol Cell Proteomics* 7(3):519-533.
6. Isserlin R, et al. (2015) Systems analysis reveals down-regulation of a network of pro-survival miRNAs drives the apoptotic response in dilated cardiomyopathy. *Mol Biosyst* 11(1):239-251.
7. Engholm-Keller K & Larsen MR (2013) Technologies and challenges in large-scale phosphoproteomics. *Proteomics* 13(6):910-931.
8. Lundby A, et al. (2013) In vivo phosphoproteomics analysis reveals the cardiac targets of beta-adrenergic receptor signaling. *Sci Signal* 6(278):rs11.
9. Scholten A, et al. (2013) Phosphoproteomics study based on in vivo inhibition reveals sites of calmodulin-dependent protein kinase II regulation in the heart. *J Am Heart Assoc* 2(4):e000318.
10. Huttlin EL, et al. (2010) A tissue-specific atlas of mouse protein phosphorylation and expression. *Cell* 143(7):1174-1189.
11. Sharma P, et al. (2015) Evolutionarily conserved intercalated disc protein Tmem65 regulates cardiac conduction and connexin 43 function. *Nat Commun* 6:8391.
12. Terrin A, et al. (2012) PKA and PDE4D3 anchoring to AKAP9 provides distinct regulation of cAMP signals at the centrosome. *J Cell Biol* 198(4):607-621.
13. Vary TC & Lang CH (2008) Differential phosphorylation of translation initiation regulators 4EBP1, S6k1, and Erk 1/2 following inhibition of alcohol metabolism in mouse heart. *Cardiovasc Toxicol* 8(1):23-32.
14. Venkatesan B, et al. (2010) EMMPRIN activates multiple transcription factors in cardiomyocytes, and induces interleukin-18 expression via Rac1-dependent PI3K/Akt/IKK/NF-kappaB and MKK7/JNK/AP-1 signaling. *J Mol Cell Cardiol* 49(4):655-663.
15. Bousset K, Henriksson M, Luscher-Firzlaff JM, Litchfield DW, & Luscher B (1993) Identification of casein kinase II phosphorylation sites in Max: effects on DNA-binding kinetics of Max homo- and Myc/Max heterodimers. *Oncogene* 8(12):3211-3220.
16. Gupta MP, Amin CS, Gupta M, Hay N, & Zak R (1997) Transcription enhancer factor 1 interacts with a basic helix-loop-helix zipper protein, Max, for positive regulation of cardiac alpha-myosin heavy-chain gene expression. *Mol Cell Biol* 17(7):3924-3936.
17. Karin M & Gallagher E (2005) From JNK to pay dirt: jun kinases, their biochemistry, physiology and clinical importance. *IUBMB Life* 57(4-5):283-295.
18. Wang Q, Lin JL, Chan SY, & Lin JJ (2013) The Xin repeat-containing protein, mXinbeta, initiates the maturation of the intercalated discs during postnatal heart development. *Dev Biol* 374(2):264-280.
19. Chou MF & Schwartz D (2011) Using the scan-x Web site to predict protein post-translational modifications. *Curr Protoc Bioinformatics* Chapter 13:Unit 13.16.
20. Keshava Prasad TS, et al. (2009) Human Protein Reference Database--2009 update. *Nucleic Acids Res* 37(Database issue):D767-772.
21. Wang Y (2007) Mitogen-activated protein kinases in heart development and diseases. *Circulation* 116(12):1413-1423.
22. Juhaszova M, et al. (2009) Role of glycogen synthase kinase-3beta in cardioprotection. *Circ Res* 104(11):1240-1252.
23. Isserlin R, Merico D, Voisin V, & Bader GD (2014) Enrichment Map - a Cytoscape app to visualize and explore OMICs pathway enrichment results. *F1000Res* 3:141.
24. Burke MA, et al. (2016) Molecular profiling of dilated cardiomyopathy that progresses to heart failure. *JCI Insight* 1(6).
25. Zhou S, et al. (2000) SKIP, a CBF1-associated protein, interacts with the ankyrin repeat domain of Notch1C to facilitate Notch1C function. *Mol Cell Biol* 20(7):2400-2410.
26. Espinosa L, Santos S, Ingles-Estevé J, Munoz-Canoves P, & Bigas A (2002) p65-NFkappaB synergizes with Notch to activate transcription by triggering cytoplasmic translocation of the nuclear receptor corepressor N-CoR. *J Cell Sci* 115(Pt 6):1295-1303.
27. Sun Z, Hamilton KL, & Reardon KF (2012) Phosphoproteomics and molecular cardiology: techniques, applications and challenges. *J Mol Cell Cardiol* 53(3):354-368.
28. Ren J, et al. (2011) Computational analysis of phosphoproteomics: progresses and perspectives. *Curr Protein Pept Sci* 12(7):591-601.
29. Morrisey EE (2010) Weary of the stress: time to put another notch in cardiomyopathy. *Circ Res* 106(7):1187-1189.
30. Rizzo P, et al. (2014) The role of notch in the cardiovascular system: potential adverse effects of investigational notch inhibitors. *Front Oncol* 4:384.
31. Ryu HW, Park CW, & Ryu KY (2014) Disruption of polyubiquitin gene Ubb causes dysregulation of neural stem cell differentiation with premature gliogenesis. *Sci Rep* 4:7026.
32. Tang Y, Boucher JM, & Liaw L (2012) Histone deacetylase activity selectively regulates notch-mediated smooth muscle differentiation in human vascular cells. *J Am Heart Assoc* 1(3):e000901.
33. Chapman G, Sparrow DB, Kremmer E, & Dunwoodie SL (2011) Notch inhibition by the ligand DELTA-LIKE 3 defines the mechanism of abnormal vertebral segmentation in spondylocostal dysostosis. *Hum Mol Genet* 20(5):905-916.
34. Wu M & Li J (2015) Numb family proteins: novel players in cardiac morphogenesis and cardiac progenitor cell differentiation. *Biomol Concepts* 6(2):137-148.
35. Fedak PW, et al. (2006) Altered expression of disintegrin metalloproteinases and their inhibitor in human dilated cardiomyopathy. *Circulation* 113(2):238-245.
36. Urbaneck K, et al. (2010) Inhibition of notch1-dependent cardiomyogenesis leads to a dilated myopathy in the neonatal heart. *Circ Res* 107(3):429-441.
37. Croqueolo A, et al. (2008) Control of the adaptive response of the heart to stress via the Notch1 receptor pathway. *The Journal of experimental medicine* 205(13):3173-3185.
38. Metrich M, et al. (2015) Jagged1 intracellular domain-mediated inhibition of Notch1 signalling regulates cardiac homeostasis in the postnatal heart. *Cardiovasc Res* 108(1):74-86.
39. Gude N & Sussman M (2012) Notch signaling and cardiac repair. *J Mol Cell Cardiol* 52(6):1226-1232.
40. D'Amato G, Luxan G, & de la Pompa JL (2016) Notch signalling in ventricular chamber development & cardiomyopathy. *FEBS J*. doi: 10.1111/febs.13773.
41. Dvorakova MC, Kruzliak P, & Rabkin SW (2014) Role of neuropeptides in cardiomyopathies.

817
818
819
820
821
822
823
824
825
826
827
828
829
830
831
832
833
834
835
836
837
838
839
840
841
842
843
844
845
846
847
848
849
850
851
852
853
854
855
856
857
858
859
860
861
862
863
864
865
866
867
868
869
870
871
872
873
874
875
876
877
878
879
880
881
882
883
884

Peptides 61:1-6.

42. Zaidi S, et al. (2013) De novo mutations in histone-modifying genes in congenital heart disease. *Nature* 498(7453):220-223.

43. Cordero-Reyes AM, et al. (2016) Full Expression of Cardiomyopathy Is Partly Dependent on B-Cells: A Pathway That Involves Cytokine Activation, Immunoglobulin Deposition, and Activation of Apoptosis. *J Am Heart Assoc* 5(1): e002484.

44. Hofmann U & Frantz S (2015) Role of lymphocytes in myocardial injury, healing, and remodeling after myocardial infarction. *Circ Res* 116(2):354-367.

45. Dobaczewski M, Chen W, & Frangogiannis NG (2011) Transforming growth factor (TGF)-beta signaling in cardiac remodeling. *J Mol Cell Cardiol* 51(4):600-606.

46. Finck BN (2007) The PPAR regulatory system in cardiac physiology and disease. *Cardiovasc Res* 73(2):269-277.

47. Vallejo JG (2011) Role of toll-like receptors in cardiovascular diseases. *Clinical Sci* 121(1):1-

10.

48. Dawson K, Aflaki M, & Nattel S (2013) Role of the Wnt-Frizzled system in cardiac pathophysiology: a rapidly developing, poorly understood area with enormous potential. *J Physiol* 591(6):1409-1432.

49. Beausoleil SA, Villen J, Gerber SA, Rush J, & Gygi SP (2006) A probability-based approach for high-throughput protein phosphorylation analysis and site localization. *Nat Biotechnol* 24(10):1285-1292.

50. Chawade A, Alexandersson E, & Levander F (2014) Normalizer: a tool for rapid evaluation of normalization methods for omics data sets. *J Proteome Res* 13(6):3114-3120.

51. Schwartz D, Chou MF, & Church GM (2009) Predicting protein post-translational modifications using meta-analysis of proteome scale data sets. *Mol Cell Proteomics* 8(2):365-379.

885
886
887
888
889
890
891
892
893
894
895
896
897
898
899
900
901
902
903
904
905
906
907
908
909
910
911
912
913
914
915
916
917
918
919
920
921
922
923
924
925
926
927
928
929
930
931
932
933
934
935
936
937
938
939
940
941
942
943
944
945
946
947
948
949
950
951
952

Submission PDF